Functional Connectivity Differences of the Subthalamic Nucleus Related to Parkinson's Disease

Christian Mathys,[1] Julian Caspers,[1,2]* Robert Langner,[2,3] Martin Südmeyer,[3,4] Christian Grefkes,[2,5] Kathrin Reetz,[2,6] Alexia-Sabine Moldovan,[3] Jochen Michely,[2,5] Julia Heller,[6] Claudia R. Eickhoff,[2,7] Bernd Turowski,[1] Alfons Schnitzler,[3,4] Felix Hoffstaedter,[2,3] and Simon B. Eickhoff[2,3]

[1]Department of Diagnostic and Interventional Radiology, Medical Faculty, University Düsseldorf, Düsseldorf, Germany
[2]Institute of Neuroscience and Medicine (INM-1, INM-3, INM-4), Research Centre Jülich, Jülich, Germany
[3]Institute of Clinical Neuroscience and Medical Psychology, Medical Faculty, University Düsseldorf, Düsseldorf, Germany
[4]Center for Movement Disorders and Neuromodulation, Department of Neurology, Medical Faculty, University Düsseldorf, Düsseldorf, Germany
[5]Department of Neurology, Neuromodulation & Neurorehabilitation Group, University of Cologne, Cologne, Germany
[6]Department of Neurology and JARA BRAIN, RWTH Aachen University, Aachen, Germany
[7]Department of Psychiatry, Psychotherapy and Psychosomatics, RWTH Aachen University, Aachen, Germany

Abstract: A typical feature of Parkinson's disease (PD) is pathological activity in the subthalamic nucleus (STN). Here, we tested whether in patients with PD under dopaminergic treatment functional connectivity of the STN differs from healthy controls (HC) and whether some brain regions show (anti-) correlations between functional connectivity with STN and motor symptoms. We used functional magnetic resonance imaging to investigate whole-brain resting-state functional connectivity with STN in 54 patients with PD and 55 HC matched for age, gender, and within-scanner motion. Compared to HC, we found attenuated negative STN-coupling with Crus I of the right cerebellum and with right ventromedial prefrontal regions in patients with PD. Furthermore, we observed enhanced negative STN-coupling with bilateral intraparietal sulcus/superior parietal cortex, right sensorimotor, right premotor, and left visual cortex compared to HC. Finally, we found a decline in positive STN-coupling with the left insula related to severity of motor symptoms and a decline of inter-hemispheric

Additional Supporting Information may be found in the online version of this article.

Contract grant sponsor: Deutsche Forschungsgemeinschaft (DFG); Contract grant numbers: EI 816/4-1, EI 816/6-1, LA 3071/3-1, GR 3285/2-1, GR3285/5-1 KFO219-TP8; Contract grant sponsor: National Institute of Mental Health; Contract grant number: R01-MH074457; Contract grant sponsor: European EFT program (Human Brain Project).

*Correspondence to: Julian Caspers, Institut für Diagnostische und Interventionelle Radiologie, Universitätsklinikum Düsseldorf, Moorenstr. 5, D-40225 Düsseldorf, Germany.
E-mail: julian.caspers@med.uni-duesseldorf.de

Received for publication 28 August 2015; Revised 12 December 2015; Accepted 13 December 2015.

DOI: 10.1002/hbm.23099
Published online 00 Month 2015 in Wiley Online Library (wileyonlinelibrary.com).

functional connectivity between left and right STN with progression of PD-related motor symptoms. Motor symptom related uncoupling of the insula, a key region in the saliency network and for executive function, from the STN might be associated with well-known executive dysfunction in PD. Moreover, uncoupling between insula and STN might also induce an insufficient setting of thresholds for the discrimination between relevant and irrelevant salient environmental stimuli, explaining observations of disturbed response control in PD. In sum, motor symptoms in PD are associated with a reduced coupling between STN and a key region for executive function. *Hum Brain Mapp 00:000–000, 2015*.

Key words: subthalamic nucleus; fMRI; brain networks; Parkinson's disease; healthy subjects

INTRODUCTION

A hallmark of patients suffering from Parkinson's disease (PD) are altered electrophysiological properties of the subthalamic nucleus (STN) due to attenuated inhibitory influences from degenerated neurons in the substancia nigra [Kuhn et al., 2009]. As a consequence, the STN is the target of current therapeutic approaches using deep brain stimulation (DBS) to suppress pathological STN activity in patients with PD. As this electrical turn-off of the STN was shown to be highly effective to ameliorate motor symptoms of PD [Rizzone et al., 2014; Volkmann, 2007], there is little doubt about the pathophysiological relevance of pathological STN activity in PD.

In the healthy brain, the STN stimulates the internal segment of the globus pallidus, leading to increased inhibition of the ventrolateral thalamus and thus increased motor inhibition (referred to as *indirect pathway*). This pathway is described as being complementary to the influence of putamen and caudate nucleus on internal globus pallidus and ventrolateral thalamus, inducing motor facilitation (*direct pathway*). Both STN and putamen as well as caudate nucleus receive excitatory input via the *hyperdirect pathway* originating from primary somatosensory cortex (S1), primary motor cortex (M1), and premotor cortical (PMC) areas [Weintraub and Zaghloul, 2013]. Key functions of the STN, with respect to motor function, include control of response thresholds [Mansfield et al., 2011], stopping of ongoing motor activity [Aron et al., 2007], and response inhibition during conflict [Brittain et al., 2012; Frank et al., 2007]. The *hyperdirect pathway* is thought to provide the sensorimotor cortex with monosynaptic control over response thresholds and other behavioral STN functions [Castrioto et al., 2014; Frank, 2006; Nambu et al., 2002]. Notably, however, the STN is not only involved in motor control but has also been implicated in cognitive and affective processing [Hamani et al., 2004; Haynes and Haber, 2013; Temel et al., 2005]. Given the rich structural connectivity of the STN, the question arises whether also functional connectivity is changed in patients with PD and -if so- how abnormal connectivity relates to clinical parameters.

Differences in resting-state networks in patients with PD have already been demonstrated and include increased functional connectivity between the rostral supplementary motor area (pre-SMA) and right M1 as well as decreased functional connectivity between pre-SMA and left putamen [Wu et al., 2011]. A more recent study described enhanced connectivity between SMA and putamen in patients with PD [Yu et al., 2013]. However, only few studies did explicitly focus on PD-related functional connectivity changes of the STN. A seed-based whole-brain resting-state functional connectivity analysis of 31 patients with PD reported increased functional connectivity of the STN with sensorimotor cortex (S1/M1) and PMC during the medication-OFF state compared to healthy controls [Baudrexel et al., 2011]. Specifically, increased functional connectivity with the hand area of S1/M1 was found in the tremor subgroup of the same study, while non-tremor patients displayed increased functional connectivity of STN with midline cortical motor areas including the SMA. A more recent study investigated functional connectivity of *a priori* defined motor areas and confirmed increased functional connectivity of STN with S1/M1 also for *de novo* (drug-naive) PD patients compared to healthy controls, suggesting that these changes occur early in the course of the disease and independent from previous dopaminergic treatment [Kurani et al., 2015]. Here, STN-S1/M1 functional connectivity values correlated positively with the Unified Parkinson's Disease Rating Scale part III (UPDRS-III; [Movement Disorder Society Task Force on Rating Scales for Parkinson's, 2003]), indicating a relevance of this connection for motor impairment.

In summary, functional connectivity between STN and S1/M1 seems to be increased in patients with PD during the medication-OFF state. It remains unclear, however, if the same is true in patients receiving dopaminergic medication, since there has been no study yet that focused on resting-state functional connectivity of the STN in the medication-ON state using BOLD-signal time-series. Although dopaminergic treatment was shown to attenuate pathological STN activity, residual pathological activity has been described even in the medication-ON state of patients with PD [Lopez-Azcarate et al., 2010]. Moreover, the aforementioned studies on functional connectivity with STN focused on positively *correlated* brain regions. This contrasts with the notion that the organization of different

TABLE I. Characteristics of the sample

Contribution site	Group	*n* (UPDRS available)	Mean age (Range)	*P* (*t*-test)	Sex: Male (%)	*P* (χ^2-test)	Measurement parameters[a]
HHU, University Hospital Düsseldorf, Germany	Controls	16 (−)	54.1 (27–81)	0.371	31.3	0.508	3 T/300/2.2/30/ 90°/3.1 × 3.1 × 3.1 mm^3
	Patients	19 (11)	57.8 (39–72)		42.1		
RWTH, University Hospital Aachen, Germany	Controls	28 (−)	63.4 (55–72)	0.464	60.7	0.336	3 T/165/2.2/30/ 90°/3.1 × 3.1 × 3.1 mm^3
	Patients	26 (26)	64.9 (39–81)		73.1		
University of Cologne, University Hospital Cologne, Germany	Controls	11 (−)	63.2 (53–74)	0.933	100	N/A	3 T/183/2.2/30/ 90°/3.1 × 3.1 × 3.1 mm^3
	Patients	9 (9)	62.9 (50–73)		100		
Overall	Controls	55 (−)	60.7 (27–81)	0.453	60.0	0.470	N/A
	Patients	54 (46)	62.1 (39–81)		66.7		

HHU, Heinrich Heine University; RWTH, Rheinisch-Westfälische Technische Hochschule.
[a]Measurement parameters: magnetic field strength of the scanner/number of continuously aquired volumes/repetition time (in s)/echo time (in ms)/flip angle/voxel size. All participants were instructed to keep their eyes closed during the measurement.

systems into *anti-correlated* (i.e., negatively coupled) networks has repeatedly been demonstrated to be a key feature of intrinsic physiological brain function. The probably best known example is negative coupling between the task-positive network (TPN), which typically shows activations during tasks that require externally directed attention, and the default-mode network (DMN), which is characterized by task-related deactivations [Fox et al., 2005; Fransson, 2005; Greicius et al., 2003; Kelly et al., 2008; Uddin et al., 2009]. This negative coupling has been discussed to represent a suppression mechanism that inhibits unwanted processes or thoughts and to increase the reliability of behavioral responses [Anticevic et al., 2012; Kelly et al., 2008; Spreng et al., 2010]. Thus, PD-related changes in networks that show negative coupling with the STN might also be relevant. Up to now, though, no study has reported changes in such networks. However, a recent study found attenuation of normal negative coupling between the dorsal attention network (DAN; which is part of the TPN) and the DMN in patients with PD with mild cognitive impairment [Baggio et al., 2015]. Interestingly, previous characterizations of the STN-correlated network reveal similarities with the TPN [Baudrexel et al., 2011; Mathys et al., 2014]. Accordingly, both the TPN and the STN-correlated network involve bilateral parts of inferior parietal cortex, dorsolateral prefrontal cortex, frontal eye field, anterior insula, frontal operculum, and preSMA/midcingulate cortex. Furthermore, both the DMN and the network which is negatively coupled with STN, involve bilateral fractions of precuneus/posterior cingulate, medial prefrontal and orbitofrontal cortex. Hence, it seems likely that PD-related changes that were reported for the TPN and DMN also involve the STN-correlated and STN-anti-correlated networks.

In this study, we therefore aimed at characterizing PD-related increases and decreases in functional connectivity with STN in brain networks that show positive or negative coupling with STN, respectively. We also sought to identify the relationships between the severity of PD-related motor symptoms and functional connectivity with STN in other brain regions. Particularly, given previous evidence for a PD-related attenuation of normal negative coupling between the TPN and DMN as well as the STN's presumed (anti-) correlations with these networks (as stated above), we predicted PD-related changes of functional connectivity with STN in TPN and DMN regions. Since many of the task-positive regions are also involved in executive functions, and most aspects of executive functioning can be compromised in PD [Kehagia et al., 2010; Michely et al., 2015], we particularly expected changes in these regions.

MATERIALS AND METHODS

Sample

Fifty-four patients with PD (31.5% females) with a mean age of 62.1 (range: 39–81) years and 55 healthy adults (40.0% females) with a mean age of 60.7 (range: 27–81) years and without any record of neurological or psychiatric disorders from three different sites were included in the current analysis (see Table I). Lateralization of motor symptoms was well balanced (see section "Assessment of PD Symptom Severity"). Written informed consent was obtained from all participants prior to inclusion. Examination at each site was approved by the local ethics committees. Approval for the joint analysis of data from all sites was obtained from the local ethics committee of the University Hospital Düsseldorf. Data of the two groups (patients and controls) were matched for age, gender, and within-scanner head-motion (see section "Data Acquisition and Preprocessing" and Table II for details). Matching was

TABLE II. Matching between groups with respect to head movement parameters

Contribution site	Group	DVARS mean (SD)	*P* (*t*-test)	FD mean (SD)	*P* (*t*-test)	RMS mean (SD)	*P* (*t*-test)
Düsseldorf	Controls	1.37 (0.27)	0.400	0.29 (0.14)	0.258	0.21 (0.11)	0.380
	Patients	1.46 (0.31)		0.35 (0.16)		0.25 (0.12)	
Aachen	Controls	1.60 (0.33)	0.790	0.35 (0.16)	0.932	0.25 (0.11)	0.805
	Patients	1.58 (0.23)		0.35 (0.11)		0.25 (0.08)	
Cologne	Controls	1.73 (0.33)	0.201	0.45 (0.17)	0.979	0.33 (0.12)	0.769
	Patients	1.90 (0.20)		0.46 (0.14)		0.32 (0.10)	
Overall	Controls	1.56 (0.33)	0.627	0.35 (0.16)	0.664	0.26 (0.12)	0.960
	Patients	1.59 (0.29)		0.37 (0.14)		0.26 (0.10)	

RMS, root mean squared movement; DVARS, derivative of RMS variance over voxels; FD, framewise displacement.

performed both in the overall sample and, importantly, also for each site. Healthy controls were selected from a large pre-existing database, which comprises many more individuals than included in this analysis. This approach allowed the close matching not only for age and gender, but also for within-scanner movement, as this parameter cannot be accounted for when recruiting subjects prior to the actual measurements.

At each site, idiopathic PD diagnosis of all patients was confirmed by clinical examination and medical history of the attending neurologist specialized for movement disorders. All patients fulfilled the standard UK Brain Bank criteria for PD [Hughes et al., 1992]. Exclusion criteria were severe dementia, major depression, contraindications for MRI, and any other physical, psychological, or medical condition that would interfere with the conduction of the study. Mean disease duration at each of the three sites was 8.2 (±5.8; Düsseldorf), 4.3 (±3.4, Aachen), and 6.6 (±3.0; Cologne). All patients received their individual PD-related medication as prescribed by the attending neurologist. Combination of Levodopa with other medications, e.g. DOPA-agonists, were also present. Mean total daily levodopa equivalent doses [Tomlinson et al., 2010] at the three sites were 801.5 (±422.2; Düsseldorf), 436.9 (±435.8; Aachen), 583.9 (±376.5; Cologne), and 592.6 (±445.9; over all sites).

Assessment of PD Symptom Severity

Motor impairment in patients with PD was assessed by items of Part III (motor part) of the Unified Parkinson's disease Rating Scale (UPDRS) [Movement Disorder Society Task Force on Rating Scales for Parkinson's, 2003]. Part III (items 18–31) evaluates several motor functions including speech, tremor, movements, rigidity, posture, gait, and bradykinesia. For our analysis, we used the sum of all Part III items (*UPDRS-III*), the sum of all left hemibody Part III items (*UPDRS-III L*; sum of items 20–26 for left hemibody) and the sum of all right hemibody Part III items (*UPDRS-III R*; sum of same items for right hemibody). At each site, the UPDRS-III items were assessed in close temporal proximity (as part of the same hospital stay and hence at most within a few days) to the MRI. UPDRS-III data (medication-ON state) was available for 46 of 54 patients. Mean UPDRS-III scores at the three sites were 12.9 (±5.6; Düsseldorf), 24.4 (±13.8; Aachen), and 12.7 (±7.7; Cologne). Lateralization of motor symptoms (according to differences between UPDRS-III L and UPDRS-III R) was well balanced: predominant to the left in 20 patients, predominant to the right in 23 patients, and symmetric in 3 patients.

Seed Definition

We defined the STN seed regions of interest (ROIs) according to an anatomical atlas generated using 7-T MRI high-resolution susceptibility mapping [Schafer et al., 2012]. The derived masks consisted of 91 voxels for left and of 89 voxels for the right STN. For the main analysis, we used a conjunction of separate left and right STN activation time series (first eigenvariate). For an additional analysis of correlation between functional connectivity with STN and motor symptoms, the first eigenvariate was derived from a common seed comprising left and right STN for robustness.

Data Acquisition and Preprocessing

Participants were instructed "not to think of anything in particular" during the scan and not to fall asleep. Patients confirmed by post-scan debriefing that they did not fall asleep. Echo-planar imaging (EPI) datasets of the entire brain (vertex to lower parts of the cerebellum) were acquired continuously on identically constructed Siemens Trio 3 T (Siemens, Erlangen) at each site, in order to record >6 min of blood oxygen level-dependent (BOLD) activity in all subjects. Except for the total number of EPIs per scan, scan parameters were identical at the three different sites (see Table I for detailed scanning parameters). However, site effects were statistically controlled for in the group-level data analysis (see below).

SPM8 (www.fil.ion.ucl.ac.uk/spm) was used for preprocessing of all datasets. To account for saturation effects, the first four images of each BOLD time series were

discarded. We used a two-pass affine registration procedure to correct for subject motion within the scanner (three translation and three rotation parameters). Images were initially realigned to the first image and then subsequently to the mean of the realigned images. In order to control for head movement, the following parameters were calculated from EPI images and the estimates of head motion generated during realignment: root mean squared movement (RMS), root mean squared signal change across time series (DVARS), and framewise displacement (FD) [Power et al., 2014; Satterthwaite et al., 2013; Van Dijk et al., 2012]. These parameters were used for movement matching between controls and patients at each site (see section "Sample" and Table II).

The mean EPI image of each subject was used for normalization to the MNI152 non-linear template (MNI, Montreal Neurological Institute) by means of the unified segmentation approach [Ashburner and Friston, 2005]. Normalization parameters were then applied to each individual EPI volume. Within the normalization procedure, image volumes were resampled to a voxel size of $1.5 \times 1.5 \times 1.5$ mm^3. A 5-mm full-width at half-maximum Gaussian kernel was afterwards applied for spatial smoothing.

Data Analysis

In order to avoid correlations explained by confounds such as physiological noise and motion, variance explained by the following parameters was removed, applying a GLM approach: (i) the six motion parameters obtained from spatial realignment (cf. above), (ii) square values of these motion parameters, (iii) the first derivatives of the six motion parameters, (iv) square values of these derivatives, and (v) global signal intensity per time-point [Jakobs et al., 2012; Reetz et al., 2012; Satterthwaite et al., 2013]. Subsequently, the data were band-pass filtered, preserving frequencies between 0.01 and 0.08 Hz [Biswal et al., 1995].

To assess resting-state functional connectivity with STN, correlation of the seed time series (provided by the first eigenvariate of all seed voxels' time series) with the time series of all other gray-matter voxels was analyzed. For each voxel, resulting Pearson correlation coefficients were then transformed into Fisher's z scores. The adjusted z scores representing STN-connectivity with each individual brain voxel were then tested for significance by a second-level analysis.

To characterize the physiologically normal STN-network in our sample, we employed an analysis of variance (ANOVA) by a general linear model (GLM) as implemented in SPM8, including non-sphericity correction, to assess STN-connectivity across both left and right STN in the group of healthy controls. Variance attributable to age, sex, and contribution site as well as their interactions was removed before statistical analysis. To investigate group differences in functional connectivity with both STN seeds between patients and controls, we explored the main effect of "group." This was performed in conjunction with the (anti-) correlated STN network in either patients or controls to constrain the analysis of group differences to regions showing correlations or anti-correlations with the STN in at least one of the two groups. That is, group differences were assessed only in those regions that were significantly connected to or negatively coupled with the STN in patients and/or controls. Significance thresholds at cluster level were adjusted by a family-wise error (FWE) correction to control for multiple comparisons and were set at $P < 0.05$ within the respective main effect mask (cluster-forming threshold at voxel level: $P < 0.001$).

Moreover, we tested for significant correlations between motor symptoms (UPDRS-III scores) and functional connectivity with STN by performing an additional second-level GLM-based analysis (same preprocessing and noise reduction as above) including those 46 (out of 54) PD patients for which UPDRS-III data were available. We tested for UPDRS-III-related differences in resting-state functional connectivity with STN. This was performed in conjunction with the significantly (anti-)correlated STN network to constrain the analysis of the UPDRS-III effect to regions showing correlation or anti-correlation with the STN. Again, results were considered significant at cluster-level FWE corrected $P < 0.05$ (cluster-forming threshold at voxel level: $P < 0.001$).

To investigate the association between function connectivity with STN and PD-related motor symptoms and to examine interactions with clinical lateralization, we extracted mean functional connectivity with left or right STN from all clusters resulting from the above analyses. Additionally, we also computed the functional connectivity between left and right STN. After variance attributable to contribution site had been removed, possible relationships (i.e., correlations) of functional connectivity values with UPDRS-III scores (total, UPDRS-III L and UPDRS-III R, cf. section "Assessment of PD Symptom Severity") were assessed. Since several combinations of connections between the resulting clusters and UPDRS-III scores were tested, this introduced an additional multiple comparison problem. Therefore, these correlations were only reported if they passed a false discovery rate (FDR)-corrected threshold of $P < 0.05$.

Anatomical assignment of resulting brain areas was performed with the SPM Anatomy toolbox (http://www.fz-juelich.de/ime/spm_anatomy_toolbox, V1.8 [Eickhoff et al., 2007]), which implements probabilistic cytoarchitectonic maps of the Jülich brain Atlas [Zilles and Amunts, 2010]. References for anatomical regions are given in Table III.

Supplementary Analysis Without Global Signal Regression

In our study, we considered global signal intensity as a nuisance variable and therefore removed it from the time-series. Although some publications warn of the possible

TABLE III. Brain areas and subregions used for anatomical assignment

Brain area	Subregions	References
Amygdala	FD, CA, SUB, EC, HATA	[Amunts et al., 2005]
Auditory cortex	TE 1.0, TE 1.1, TE 1.2	[Morosan et al., 2001]
Broca's area	BA 44, BA 45	[Amunts et al., 1999]
Cerebellum	18 structures	[Diedrichsen et al., 2009]
Hippocampus	CM, LB, SF	[Amunts et al., 2005]
Inferior parietal cortex	PFt, PF, PFm, PFcm, PFop, PGa, PGp	[Caspers et al., 2006, 2008]
Insula	Ig1, Ig2, Id1	[Kurth et al., 2010a]
Intraparietal sulcus	hIP1, hIP2, hIP3	[Choi et al., 2006; Scheperjans et al., 2008a,b]
Parietal operculum	OP 1, OP 2, OP 3, OP 4	[Eickhoff et al., 2006a,b]
Premotor cortex	BA 6	[Geyer, 2004]
Primary motor cortex	BA 4a, BA 4p	[Geyer et al., 1996]
Primary sensory cortex	BA 3a, BA 3b, BA 1, BA 2	[Geyer et al., 1999, 2000; Grefkes et al., 2001]
Superior parietal cortex	5Ci, 5L, 5M, 7A, 7M, 7P, 7PC	[Scheperjans et al., 2008a,b]
Visual cortex	BA 17 (V1), BA 18 (V2), hOC5, hOC3v (V3v), hOC4v (hV4)	[Amunts et al., 2000; Malikovic et al., 2007; Rottschy et al., 2007]

Anatomical brain areas are displayed in alphabetical order.

detrimental effects of global signal regression [Murphy et al., 2009], there is still no consensus on what is the most valid approach [Keller et al., 2013; Power et al., 2014, 2015; Zarahn et al., 1997]. However, it has been shown that global signal regression can affect the distribution of between group differences [Saad et al., 2012, 2013]. Therefore, we repeated the above-described investigation of group differences in functional connectivity with both STN between patients and controls, but this time omitted global signal regression. Only white matter and cerebrospinal fluid were used as noise-confounds [Power et al., 2014, 2015].

Supplementary Analysis on the Effect of Common or Separate STN Seeds

We used two different methods for defining the STN seeds in our investigation of group differences (conjunction of separate left and right STN seeds) and in the analysis on correlations between functional connectivity with STN and UPDRS-III scores (common seed for left and right STN). The rationale behind this was to use a more conservative approach (conjunction) for the analysis with the larger sample size (investigation of group differences) and a more robust and sensitive approach (common seed) for the analysis with the smaller sample size (UPDRS-III correlation). However, we were interested whether our results would change if the other method (for each analysis) were used. Therefore, we repeated both analyses, but this time used a common seed for the investigation of group differences and we used a conjunction of separate left and right STN seeds for detection of correlation between functional connectivity with STN and UPDRS-III.

Supplementary Analysis on Regions With Age-Related Changes of Functional Connectivity With STN

Regarding brain regions showing age-effects on functional connectivity with STN in healthy subjects [Mathys et al., 2014], we also tested for group differences in functional connectivity with left or right STN between patients and controls. Second, we analyzed whether previously described age-related effects on functional connectivity with STN can be confirmed across our entire sample of both, PD patients and healthy controls (see Supporting Information for more details).

RESULTS

Whole-Brain Functional Connectivity Pattern of the STN

Testing for bilateral functional connectivity with STN across healthy controls revealed significant positive coupling between STN and a broad network of subcortical and cortical areas (Fig. 1). At the subcortical level, we found significant resting-state connectivity bilaterally to the putamen, caudate nucleus, globus pallidus, thalamus, hippocampus (areas EC, HATA) as well as midbrain and pons. At the cortical level, significant positive STN connectivity was found bilaterally to the anterior and mid-cingulate cortex, anterior, posterior and mid-insula, dorsolateral prefrontal cortex, Broca's area, frontal and parietal operculum, auditory cortex, primary visual cortex (V1; area 17), inferior parietal cortex, intraparietal sulcus, S1, M1, and PMC. Finally, we found cerebellar connectivity in lobules I–VI, bilaterally.

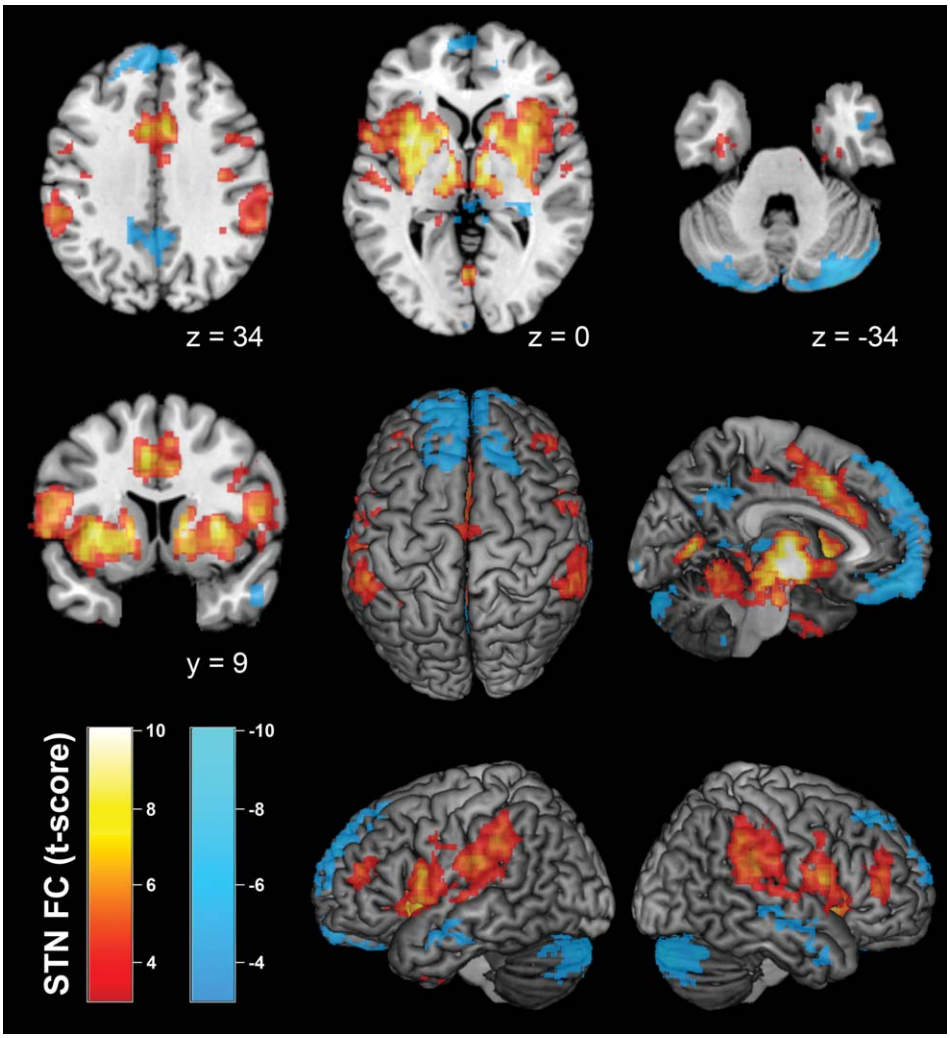

Figure 1.

Resting-state functional connectivity of the bilateral STN seed region across healthy controls. Positive network coupling is denoted in warm colors, while cold colors denote negatively coupled regions. Montreal Neurological Institute coordinates are provided for transsectional slices. Surface rendering was performed with MRIcron [Rorden and Brett, 2000]. A conjunction of left and right STN seeds was used for data analysis. [Color figure can be viewed in the online issue, which is available at wileyonlinelibrary.com.]

Negatively coupled, i.e. anti-correlated, regions identified by significant negative connectivity comprised bilateral orbitofrontal cortex, precuneus/posterior cingulate, superior frontal gyrus, middle temporal gyrus, hippocampus (areas CA, SUB), and cerebellum (lobules VI, VIIa, and IX bilateral). More detailed information on correlated and negatively coupled regions (including allocation to probabilistic cytoarchitectonic maps) is provided as Supporting Information.

In accordance with previous characterizations of the STN's functional network [Baudrexel et al., 2011; Mathys et al., 2014] there are similarities between STN-correlated regions and the TPN as well as between negatively STN-coupled regions and the DMN. Accordingly, both, TPN und STN-correlated network, involved fractions of inferior parietal cortex, dorsolateral prefrontal cortex, insula, frontal and parietal operculum, and preSMA/midcingulate cortex, each bilaterally. Furthermore, both, DMN and the network, which is negatively coupled with STN, involved fractions of precuneus/posterior cingulate, medial prefrontal and orbitofrontal cortex, each bilaterally.

Group Differences in Functional Connectivity With STN Between Patients and Controls

No significant group differences in resting-state functional connectivity (neither increases nor decreases of

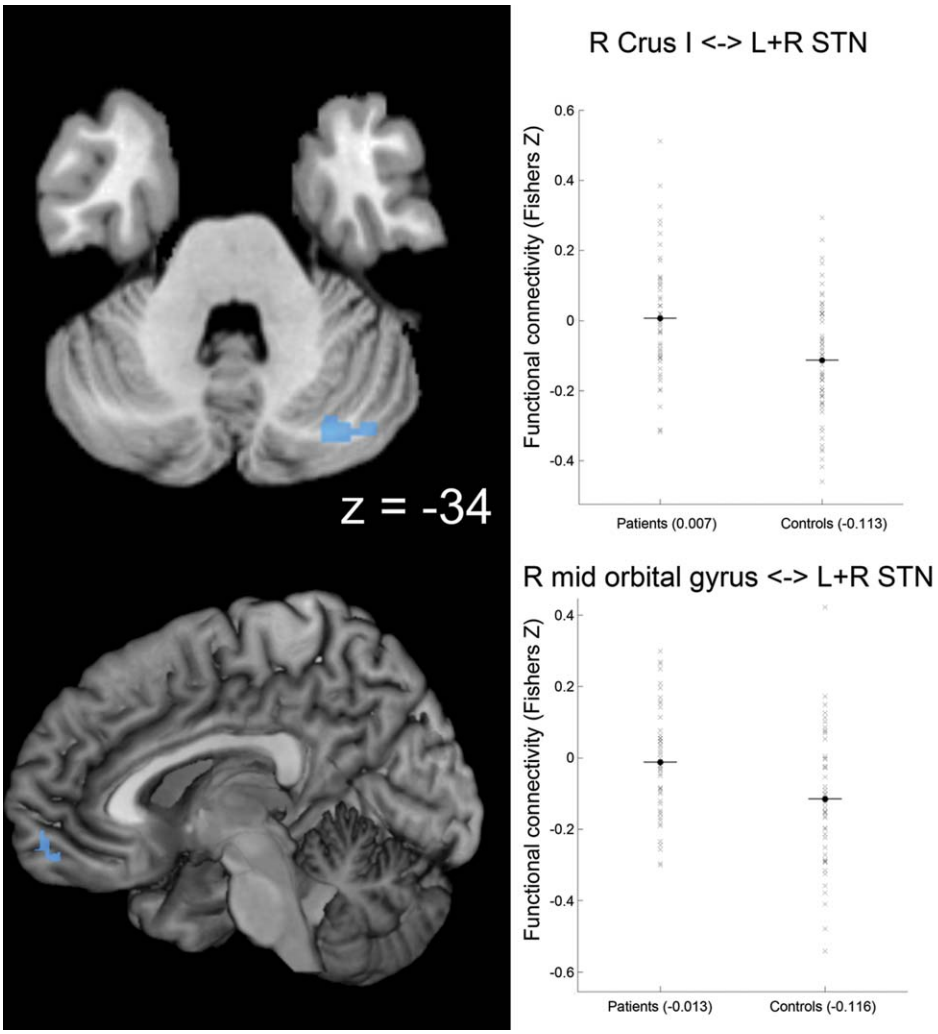

Figure 2.

Attenuated negative coupling with STN in Parkinson patients. Clusters showing a significant PD-related attenuation of negative coupling (i.e., functional connectivity in patients > controls and functional connectivity negative in controls) with the seed region (i.e., bilateral STN) are marked in cold colors. Coordinates refer to Montreal Neurological Institute space. Surface rendering was performed with MRIcron [Rorden and Brett, 2000]. Scatter plots for right Crus I of the cerebellum (R Crus I) and for right (R) mid-orbital gyrus show functional connectivity with STN for patients and controls. A conjunction of left and right STN seeds was used for data analysis. [Color figure can be viewed in the online issue, which is available at wileyonlinelibrary.com.]

functional connectivity values) with STN related to PD were found in the positively coupled STN-network, including the connection between left and right STN. In turn, we found both *attenuation* and *enhancement of negative coupling* with the STN (explanations for both terms below).

First, we found significantly reduced negative functional connectivity with STN in patients with PD compared to healthy controls (i.e., functional connectivity in patients > controls AND functional connectivity negative in controls) in right lobule VII a Crus I of the cerebellum, right mid-orbital gyrus, and right rectal gyrus. Here, the functional connectivity values of the respective clusters in the patient group were close to zero. Hence, we consider these clusters as brain areas with *attenuated negative STN-coupling* in patients with PD (Fig. 2 and Table IV).

Second, we observed significantly increased negative functional connectivity with STN in patients with PD compared to healthy controls (i.e., functional connectivity in patients < controls AND functional connectivity negative in patients) with bilateral intraparietal sulcus (IPS; area hIP3), bilateral SPC (bilateral 7A, bilateral 7PC, right 7P), bilateral S1, and left visual cortex (V1, V2). As detailed in Table IV, functional connectivity values of these regions in the control group were close to zero. We therefore regard

TABLE IV. Differences between patients and controls in intrinsic functional connectivity with both STNs

	Pair of regions	Coordinates $x/y/z$ (mm)	Mean $Z_{controls}$	Mean $Z_{patients}$	P	d'
Enhanced negative STN-coupling in PD patients	L+R STN–L IPS/SPC/S1	−40/−48/56	0.019	−0.143	0.0001	−0.77
	L+R STN–R SPC	24/−64/62	0.008	−0.127	0.0003	−0.72
	L+R STN–R S1	34/−38/64	0.005	−0.144	0.0001	−0.78
	L+R STN–R IPS/SPC/S1	34/−48/50	0.012	−0.142	0.0001	−0.76
	L+R STN–L V1/V2	−4/−94/14	−0.004	−0.116	0.0011	−0.64
Attenuated negative STN-coupling in PD patients	L+R STN–R Crus I	28/−76/−36	−0.113	0.007	0.0004	0.69
	L+R STN–R mid orbital/rectal gyrus	8/58/−10	−0.116	−0.013	0.0015	0.63

Mean $Z_{controls}$ and $Z_{patients}$ denote group-averaged functional connectivity in 55 healthy participants and 54 patients with Parkinsons's disease (PD); d' denotes the effect size according to Cohen's definition [Cohen, 1988]. STN, subthalamic nucleus; SPC, superior parietal cortex; S1, primary sensory cortex; IPS, intraparietal sulcus; V1 and V2, subregions (area 17 and 18) of the visual cortex; L, left; R, right; Crus I is part of cerebellar lobule VIIa.

these clusters as regions showing *enhanced negative STN-coupling* in patients with PD (Fig. 3 and Table IV). Notably, the clusters involving the IPS and SPC bilaterally correspond to coordinates of the TPN as provided by Fox et al. [2005].

Correlation Between Motor Symptoms and Functional Connectivity With STN

We performed an additional group-level ANOVA, including 46 patients with PD with available UPDRS data, to test for associations of UPDRS-III scores and functional connectivity with STN. Here, we observed a significant *positive* correlation between motor symptom severity (UPDRS-III) and functional connectivity with STN in a region at the border between S1 and SPC (7PC) on the left hemisphere (Fig. 4). There was also a trend toward significance ($P = 0.055$; after correction) for a contralateral corresponding cluster within the right SPC (7PC, 7A). Of note, on both hemispheres, these clusters overlapped with the "enhanced negative STN-coupling" clusters in patients with PD as detailed in section "Group Differences in Functional Connectivity with STN Between Patients and Controls." These regions thus show zero correlation in healthy subjects (Table IV) and negative STN-coupling in patients, which, however, declines back to zero (i.e., toward the physiological state) in more severely affected individuals (Figs. 3 and 4). On the other hand, we found a significant *negative* correlation between UPDRS-III and functional connectivity with STN of left mid-insula (Fig. 4). That is, the STN was weaker coupled to this region in more severely affected patients.

In the next step, a set of *analyses* was performed to assess potential relationships between clinical lateralization of the motor symptoms and functional connectivity with STN at the clusters showing (anti-) correlation with UPDRS-III scores (L S1/SPC, R SPC, L insula) and the clusters featuring group differences in functional connectivity with STN (L IPS/SPC, L V1/V2, R IPS/SPC/S1, R M1/PMC, R mid orbital/rectal gyrus, R Crus I; Table IV). For this purpose, we tested correlations between all combinations of left/right functional connectivity with STN and UPDRS-III motor scores (sum score, L and R, as described in section "Assessment of PD Symptom Severity"). We found a significant ($P = 0.002$ after FDR correction, $r = -0.44$) negative correlation between functional connectivity of left mid-insula (for which the additional ANOVA had demonstrated *negative* correlation between UPDRS-III and functional connectivity with STN) with left STN and right-sided motor symptoms (UPDRS-III R; see Fig. 4). No other combinations of the mentioned motor scores and *left functional connectivity with STN* or *right functional connectivity with STN* for all nine clusters revealed a significant correlation in this analysis. This was also true for left S1 and right SPC (for which the additional ANOVA had demonstrated *positive* correlation between UPDRS-III and functional connectivity with STN).

Functional connectivity between left and right STN was anti-correlated ($P = 0.015$ after FDR correction, $r = -0.36$) with the total UPDRS-III (Fig. 5). Significant correlations with the hemibody-specific UPDRS L or UPDRS R scores, in turn, were not observed.

Summary on Supplementary Findings Related to the Effect of Global Signal Regression

To analyze, whether group differences in functional connectivity with STN between patients and controls might have been introduced by global signal regression, we repeated this analysis without global signal regression but only removed white matter and cerebrospinal fluid signals. In summary, we could confirm all group differences between patients and controls with respect to functional connectivity with STN. The only exception was attenuated negative coupling in right mid orbital gyrus. Hence, we can exclude that the main results of our study are just artifacts that were introduced by global signal regression.

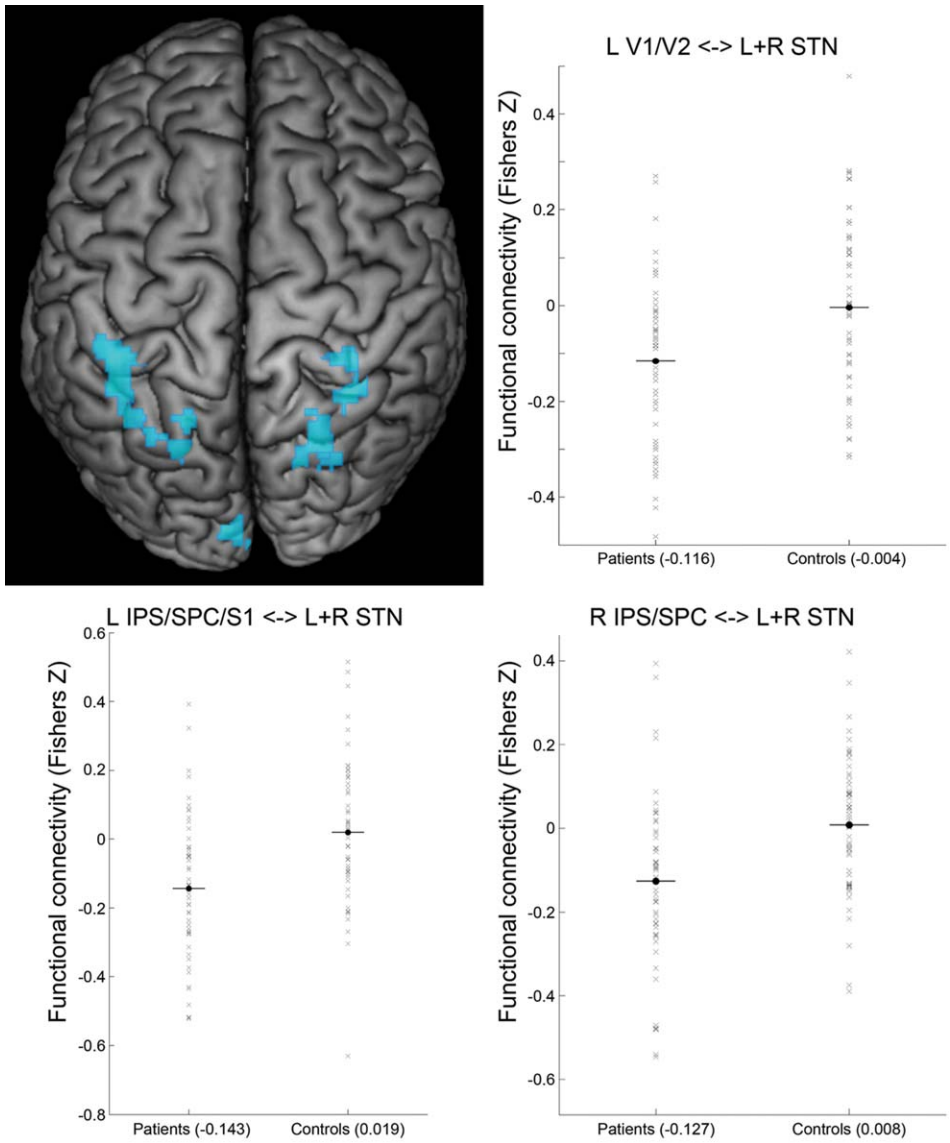

Figure 3.

Enhanced negative coupling with STN in Parkinson patients. Clusters showing a significant PD-related enhancement of negative coupling (i.e., functional connectivity in patients < controls and functional connectivity negative in patients) with the seed region (i.e., bilateral STN) are marked in cold colors. Surface rendering was performed with MRIcron [Rorden and Brett, 2000]. Scatter plots show functional connectivity of STN (Fisher's *Z*) with left areas 17 + 18 of visual cortex (L V1/V2), left intraparietal sulcus/superior parietal/somatosensory cortex (L IPS/SPC/S1) and right intraparietal sulcus/superior parietal cortex (R IPS/SPC) for patients and controls. A conjunction of left and right STN seeds was used for data analysis. [Color figure can be viewed in the online issue, which is available at wileyonlinelibrary.com.]

Summary on Supplementary Findings Related to the Effect of Common or Separate STN Seeds

Because we used two different methods for defining the STN seeds (common seed for left and right STN or conjunction of two separate seeds) in our study, we performed some supplementary analyses. Nearly all of the clusters showing group differences between patients and controls (only exception: attenuated negative coupling in right mid orbital gyrus) could be confirmed when a common STN seed was used instead of the conjunction approach. As expected, however, most of the resulting clusters were larger, when the common seed approach was applied. This was particularly noticeable for the

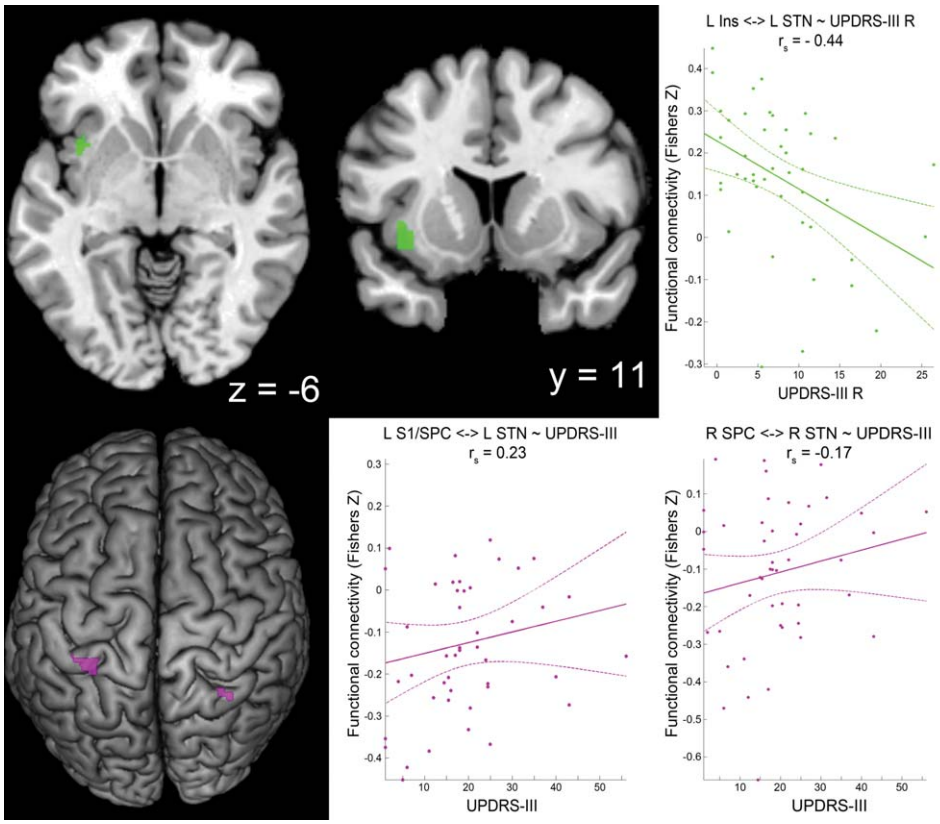

Figure 4.

Correlation of UPDRS-III motor scores and functional connectivity with STN. Clusters showing correlation between functional connectivity with STN and Unified Parkinson's Disease Rating Scale part III (UPDRS-III) values are marked in green (negative correlation) and violet (positive correlation) colors. Only left (L) mid-insula (Ins) and L somatosensory cortex (S1)/superior parietal cortex (SPC) clusters survived significance thresholds after correction, while there was only a trend toward significance [$P_{corr} = 0.053$] for the cluster at right (R) SPC. Coordinates refer to Montreal Neurological Institute space. Surface rendering was performed with MRIcron [Rorden and Brett, 2000]. The scatter plots show the individual functional connectivity (between clusters and left or right STN) against UPDRS-III scores for the right hemibody (UPDRS-III R) or for the total UPDRS-III score (UPDRS-III) across a patient subgroup ($n = 46$) with available UPDRS-III data. Linear regression line with 95% confidence interval (dotted lines), as well as r_s-values (Spearman's rank correlation coefficient) are provided. A singular seed (comprising left and right STN) was used for the general linear model approach, but separate (left and right STN) seeds were used for calculation of the scatter plots. [Color figure can be viewed in the online issue, which is available at wileyonlinelibrary.com.]

clusters showing enhanced negative coupling with STN in patients and additional clusters with enhanced negative coupling found in right M1 and right PMC. For the correlation analysis, using a conjunction of left and right STN instead of a common seed also revealed negative correlation between UPDRS-III and functional connectivity between the STN and left insula. However, positive correlation between UPDRS-III and functional connectivity between the STN and left S1 as well as right SPC were likewise present but did not survive significance thresholding any more. We would therefore argue that the conjunction of left and right STN seeds is a more conservative and potentially more specific approach, which seems suitable for detecting group differences in the whole sample. In turn, the common seed approach is more sensitive and should hence be the right choice for the smaller sample that was used for the correlations with UPDRS-III scores.

Summary on Supplementary Findings for Regions with Age-related Changes of Functional Connectivity with STN

Most of the age-related changes of functional connectivity with STN we had previously described [Mathys et al., 2014], could be confirmed in our present sample (including patients and controls). We found positive correlations between age and functional connectivity with STN for left putamen and left precuneus. Also in agreement with our

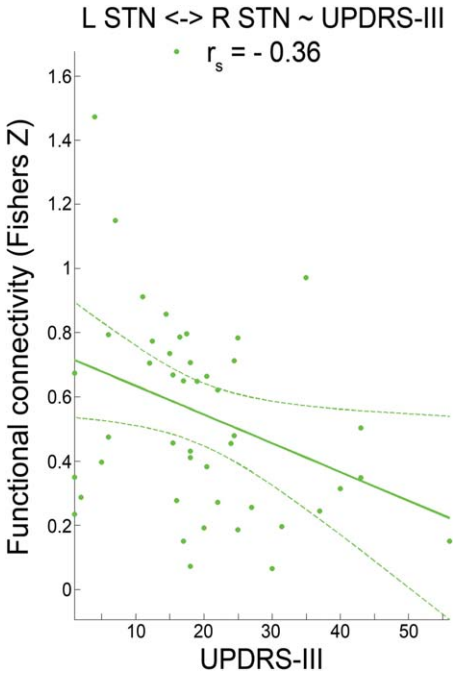

Figure 5.

Correlation of UPDRS-III motor scores and functional connectivity between left and right STN. Scatter plot shows the individual functional connectivity between left and right STN against Unified Parkinson's disease Rating Scale part III (UPDRS-III) values across a patient subgroup ($n = 46$) with available UPDRS-III data. Linear regression line with 95% confidence interval (dotted lines), as well as r_s-values (Spearman's rank correlation coefficient) are provided. [Color figure can be viewed in the online issue, which is available at wileyonlinelibrary.com.]

previous findings, we observed a negative correlation between age and functional connectivity with STN for right posterior insula, right thalamus, and caudate nucleus. However, we could not replicate the previously observed positive correlations between age and functional connectivity with STN with a region in right sensorimotor cortex. This most likely was due to oppositional age effects on functional connectivity between patients and controls in this region (details are provided as Supporting Information).

DISCUSSION

The STN plays a central role in both, pathophysiology and targeted invasive treatment of PD. In our analysis, we found complex PD-related changes in the STN-network when patients were under the regular medication-ON state. In line with our hypotheses, we found PD-related changes in functional connectivity with STN within the (anti-)correlated STN-network. In particular, we observed a PD-related attenuation of functional network distinction between STN and right Crus I of the cerebellum, right mid-orbital and right rectal gyrus. Furthermore, we found enhanced negative STN-coupling with IPS, SPC, S1, and V1/V2 in patients with PD. Notably, bilateral IPS and SPC correspond to regions of the TPN matching the stereotaxic coordinates provided by Fox et al. [2005]. Moreover, we observed a decline in positive STN-coupling with the left insula with progression of motor symptoms in patients. Finally, we found a decline of inter-hemispheric functional connectivity between left and right STN with progression of PD-related motor symptoms.

PD-Related Differences in Negative Functional Connectivity With the STN

Attenuated negative STN-coupling

We observed a PD-related attenuation of negative coupling between the STN and lobule VIIa Crus I of the cerebellum. Of note, there is clear evidence that this part of the cerebellum is not involved in motor functions but rather plays a role in cognitive processes. A recent study used Meta-Analytic Connectivity Modeling (MACM) on data of 1,359 neuroimaging experiments to link behavioral domains to different cortico-cerebellar connectivity patterns [Balsters et al., 2014]. Crus I+II were characterized by co-activations with prefrontal and parietal cortices. These prefrontal-parietal-cerebellar (Crus I+II) circuits were more active during cognitive tasks including attention and working memory [Balsters et al., 2014]. In this context, it is interesting that cerebellar pathology in PD, such as altered resting-state functional connectivity of the dentate nucleus [Liu et al., 2013] and a decrease in resting-state brain activity in (left) cerebellar lobule VII [Skidmore et al., 2013], has been reported repeatedly. Additionally, in patients with non-demented PD with impaired cognition (based on the Clinical Dementia Rating), reduced regional gray-matter volume in the cerebellum was reported ([Nishio et al., 2010]; see also [Wu and Hallett, 2013] for review). Besides other cognitive performance impairments, dual-task performance was shown to be impaired in patients with PD [Rochester et al., 2014; Wild et al., 2013]. Interestingly, the cerebellum has been previously found to be involved in dual-tasking, and its proposed role was to efficiently integrate motor and cognitive networks [Wu et al., 2013]. Notably, dual-tasking ability has an impact on quality of life in patients with PD [Klepac et al., 2008]. Considering this background, it seems important to clarify the neurobiological underpinnings of PD-related dual-task interference. Since we observed a PD-related attenuation of functional network distinction between STN and right Crus I, it is tempting to speculate that, compared to healthy subjects, PD patients suffer from an increased interference between cognitive processing and processing in the STN motor network. Potentially, this interference (i.e., dedifferentiation; cf. [Roski et al., 2013]) might underlie the above-mentioned impaired performance during simultaneous motor and cognitive task execution. The

effect on functional connectivity we observed in Crus I did not show a significant correlation with motor symptoms. This would fit with the non-motor functions discussed above. However, no direct evidence was found in the literature supporting the hypothesis that changes in resting-state functional connectivity at cerebellar Crus I correspond to cognitive decline in patients with PD. And since cognitive performance was not assessed in our sample, this potential relationship needs to be investigated in future studies. We also observed an attenuation of functional network distinction between STN and ventro-medial prefrontal cortex (right mid-orbital and rectal gyrus). Though, we could not confirm this finding, when global signal regression was omitted (see section "Summary on supplementary findings related to the effect of global signal regression"). Therefore, we cannot exclude that this specific result is just an artifact that was introduced by global signal regression.

Enhanced negative STN-coupling in PD

Bilateral IPS/SPC showed enhanced negative STN-coupling in patients with PD. As mentioned previously, the negatively STN-coupled network shows similarities with the DMN. Obviously, this network seems to show a PD-related expansion to bilateral IPS/SPC. Of note, in healthy individuals, the IPS/SPC is typically involved in the DAN, which in turn is part of the TPN [Fox et al., 2005]. Hence, our findings suggest that in PD IPS/SPC segregate (i.e., reduce coupling) from the DAN and show more correlation with the DMN. These findings are in line with previous results from patients with PD in medication-ON state, who displayed an attenuation of negative coupling between DMN and TPN [Rektorova et al., 2014]. There, the authors speculated that this decline might underlie the characteristic impairment of attention in PD. A second study described an association between attenuation of normal negative DAN-DMN-coupling and mild cognitive impairment in patients with PD [Baggio et al., 2015]. Another recent study detected decreased positive coupling between hubs of the Ventral and Dorsal Attention Networks in patients with PD who suffered from increased visual misperception, which is a known phenomenon in PD [Shine et al., 2014]. The hypothesis on PD-related conversion of the IPS/SPC region from the TPN toward the DMN is also supported by previous descriptions of this region as a part of the central executive network (CEN) [Seeley et al., 2007]. Although this network typically is physiologically anti-correlated to the DMN during rest, the CEN shows significantly increased positive coupling with the DMN in patients with PD [Putcha et al., 2015]. However, canonical networks like DMN and TPN have not been systematically defined in this analysis. Therefore, attempts to assign the effects in our study to PD-related changes of large-scale resting-state networks need to be examined in future studies, using data-driven definitions of these networks (e.g., via independent component analysis).

Another special feature of the SPC is its involvement in spatial aspects of motor planning [Grefkes et al., 2004]: the region showed increased brain activity during sequential (but not repetitive) movement tasks in positron emission tomography (PET) studies [Catalan et al., 1998; Winstein et al., 1997]. In Brodmann area 7 of the SPC, another PET study found abnormally increased brain activity with higher task complexity in patients with PD [Catalan et al., 1999]. Furthermore, parietal cortex activity in healthy participants was reported in association with word naming, also becoming stronger with increasing naming difficulty [Binder et al., 2005]. Since sequencing is also a relevant aspect in speech production, a recent analysis focused on determining sequencing-related brain regions that are shared in speech production and finger movement [Heim et al., 2012]. The authors observed that left area 7A of SPC is responsible for general aspects of motor sequencing during both hand actions and speech production. Notably, when generating affective prosody, patients with PD showed over-activation, relative to healthy controls, in left area 7A of SPC [Arnold et al., 2013]. This previous evidence supports the assumption that SPC, especially subregion 7A, is involved in compensatory processes (related to impaired sequencing, e.g., in speech production) in patients with PD. To speculate, the known PD-related pathological STN-activity [Kuhn et al., 2009] might compromise normal functioning of other brain-regions in the STN-network. It is therefore conceivable that PD-related negative coupling between STN and SPC serves in a compensatory manner, namely by preventing interference from pathological STN-activity on SPC activity. Of note, functional connectivity with STN of a right SPC-cluster correlated (only trend towards significance) with motor symptoms. This region thus shows zero connectivity with STN in healthy subjects and enhanced negative STN-coupling in patients but declines back to zero correlation (i.e., toward the physiologically normal state) in more severely affected individuals. This can be interpreted as a compensatory effect, which is present in less affected patients and breaks down in more affected patients. It needs to be reemphasized, however, that the concept of compensatory negative coupling with STN is speculative. Network organization might differ when in the active state compared to the resting-state condition. Our interpretation, therefore, needs to be addressed in future studies, employing a broad range of behavioral tests including motor sequencing and speech production. Furthermore, it is not clear how PD-related alterations in alpha and beta band oscillations (8–35 Hz) of STN local field potentials [Kuhn et al., 2009] relate to very low frequency oscillations in BOLD time series. The assumption of at least some degree of relationship between both signals is supported by simultaneous recordings of BOLD signal and local field potentials during spontaneous activity in early visual

cortices of monkeys. Although gamma band oscillations (40–100 Hz) of local field potentials were most informative about BOLD fluctuations, both alpha and beta power signals carried additional information about the BOLD signal [Magri et al., 2012].

To summarize our considerations on PD-related enhanced negative STN-coupling, we would interpret these findings as a segregation of the task-positive DAN (IPS/SPC) or as an expression of compensatory mechanisms (related to impaired sequencing, e.g., in speech production) in PD, and enhanced negative coupling might be a way to protect compensatory brain regions from interference through pathological activity of the STN.

Functional Connectivity Between Left and Right STN

While PD-related negative STN-coupling of IPS/SPC was mostly driven by patients with less severe motor symptoms (i.e., it was virtually absent in healthy controls as well as in patients with more pronounced symptoms), the normal positive coupling between left and right STN decreased in patients with increasing motor impairment. The presence of structural and functional connections of STN with the contralateral hemisphere has been demonstrated for both subcortical (e.g., putamen) and cortical structures [Brunenberg et al., 2012]. However, to our knowledge, no direct inter-hemispheric structural connections have been reported between left and right STN. This supports the hypothesis that a functional connection with relatively high functional connectivity values between left and right STN (see Results section) is established despite an unknown amount of synaptic relays within this connection. Known structural connections of bilateral STN to bilateral subcortical (putamen and caudate nucleus) and cortical (anterior and posterior cingulate cortex) regions [Brunenberg et al., 2012] might represent such relay locations but could also provide a common driving input to both STN. Previous data on functional connections between left and right STN were predominantly based on local field potential recordings from DBS electrodes in patients with PD. Nonetheless, these connections were mainly interpreted as physiological connections [Darvas and Hebb, 2014; Hebb et al., 2012; Novak et al., 2009; Walker et al., 2011]. In particular, bilateral symmetric STN power modulations of beta frequency oscillations during language and motor tasks have been reported [Hebb et al., 2012]. Activation of this bilateral network has been described even by unilateral motor programs [Darvas and Hebb, 2014]. It remains an open question if synchrony in local field potential recordings as well as resting-state functional connectivity between left and right STN reflects the same neurobiological process. If so, our observation of functional connectivity decline between bilateral STN with progression of motor symptoms might indicate dysfunction of the bilateral STN-associated motor network.

(Absence of) PD-Related Changes in Positive Functional Connectivity Between STN and S1/M1

Notably, increased resting-state functional connectivity between STN and S1/M1 was a recurrent finding in previous reports on patients in the medication-OFF state and drug-naïve PD patients [Baudrexel et al., 2011; Kurani et al., 2015]. However, our seed-based whole-brain connectivity analysis did not reveal changes in the positive coupling between STN and S1/M1 in our sample of patients with PD in the medication-ON state. As a possible explanation, we observed (in a supplementary analysis) that functional connectivity between STN and S1/M1 was influenced by an interaction between group and age. The previously described increased functional connectivity between STN and S1/M1 was only found in younger patients. Across older patients, however, the functional connectivity decline between S1/M1 and STN is exactly the opposite to what was described for patients with PD in the medication-OFF state [Baudrexel et al., 2011]. From our point of view, this is a strong indication for a dopaminergic modulation of the connection between STN and S1/M1. To our knowledge, there has been no study yet that focused on dopaminergic modulation of resting-state functional connectivity between STN and sensorimotor cortex using BOLD-signal time-series. On the other hand, a recent analysis of functional connectivity with STN using arterial spin-labeled perfusion fMRI found a weak positive correlation between functional connectivity of STN with left M1 and levodopa dose [Fernandez-Seara et al., 2015]. However, even if the dopaminergic medication in our sample were the explanation for not observing increased positive coupling between STN and S1/M1 the neurobiological substrates of this coupling would still be unclear. At least two explanations are worth considering: First, it could be a cause of pathophysiological changes, which might be effectively antagonized by medical treatment. More precisely, increased functional connectivity between STN and M1 in the medication-OFF state might be driven by pathological activity of the STN, but the effect could be attenuated in the medication-ON state. Second, the increased functional connectivity between STN and S1/M1 in the medication-OFF state could be part of a compensatory mechanism that becomes unnecessary under medication. For a better understanding of how STN connectivity is influenced by dopaminergic treatment, future studies on resting-state functional connectivity of the STN should include scans under both conditions (medication-ON and -OFF state) from the same patients.

PD-Related Changes in Positive Functional Connectivity Between STN And Insula

Functional connectivity between the left mid-insula and the STN declined in patients with PD with more severe

motor symptoms. According to a hierarchical model of the human insula, sensorimotor information initially reaches the posterior part of the insular cortex and is afterwards integrated at its anterior part with emotional and cognitive evaluations [Craig, 2009; Kurth et al., 2010b]. Moreover, the insula is thought to play a superordinate role in the interaction between motor, cognitive, and affective functions [Kelly et al., 2012; Kurth et al., 2010b]. In this context it does not come as a surprise that the anterior insula has been identified as a key region for executive functioning [Cieslik et al., 2015; Müller et al., 2015]. Interestingly, several mental disorders are associated with gray-matter atrophy of the anterior insula, and atrophy seems to be correlated with executive dysfunction [Goodkind et al., 2015]. In PD, insular atrophy is a well-known phenomenon [Ibarretxe-Bilbao et al., 2010, 2011; Shine et al., 2014; Yamamoto et al., 2007]. Furthermore, reduced activation of the anterior insula during working memory (a key component of executive function) tasks in PD has been reported [Rottschy et al., 2013]. Another key component of executive function is inhibitory control [Müller et al., 2015], which is also a function the STN is involved in [Aron et al., 2007; Mansfield et al., 2011]. Taken together, the connection between STN and insula could be important for different aspects of executive functioning, and our observation of PD-related decline in functional connectivity within this connection might contribute to previously reported executive dysfunctions in PD [Rottschy et al., 2013; Shine et al., 2014; Ye et al., 2014].

Compatible to its important role for executive functions, the insula has also been identified as an integral hub of the so-called salience network [Menon and Uddin, 2010; Seeley et al., 2007; Shulman et al., 2009]. It has been proposed that the insula is not only involved in detection of salient stimuli but also in switching between other large-scale networks in order to assist target brain regions in generating appropriate behavioral responses [Menon and Uddin, 2010]. Considering the typical STN-functions (mediating response conservativeness and conflict resolution), the symptom-related decoupling between insula and STN might lead to impaired thresholds for identification of relevant, or suppression of irrelevant, salient environmental stimuli at the insular level. Hence, PD-related motor symptoms might, at least partially, rely on inadequate insular processing of sensorimotor information, potentially caused by decline of functional connectivity between STN and insula. A recent study illustrates the relationship between PD-related motor symptoms and disturbed response control [Matar et al., 2013]. Here, PD patients, particularly when affected by freezing-of-gait, displayed deficits in conflict resolution (inhibition of implicitly cued behavior) and increased susceptibility to salient environmental triggers. Besides these possible influences by the STN on insular function, the reverse direction of influence might be true. As a higher-order control region, the insula might just loose functional connectivity with an important interface (i.e., STN) for the realization of motor inhibition, which might be triggered by uncontrolled pathological STN-activity [Kuhn et al., 2009]. Insular atrophy might therefore just represent degeneration secondary to breakdown of functional connectivity with a target region. In summary, uncoupling between insula and STN might induce insufficient setting of thresholds for discriminating between relevant and irrelevant salient environmental stimuli.

Limitations and Future Directions

Some limitations of our analysis might derive from the multi-site approach. Although all healthy controls were without any record of neurological or psychiatric disorders, and patients with PD were diagnosed according to standardized diagnostic criteria, there may be subtle differences in screening and characterization between sites. Furthermore, subject groups across sites were not completely homogenous. Particularly, patients at Aachen were more severely affected (higher UPDRS-III-values) than in Cologne or Düsseldorf. Benefits of a multi-site approach, however, include a substantially larger sample size and ensuing higher statistical power. In addition, this approach may yield an enhanced generalizability of the results, because pooling of data from potentially different patient populations and clinical predilections in the different hospitals enable a more realistic assessment of the overall population of PD patients, despite potentially increased nuisance variance of the data.

Complementing previous studies that investigated resting-state functional connectivity with STN in the medication-OFF state of patients [Baudrexel et al., 2011; Kurani et al., 2015], this study analyzed patients with PD under dopaminergic treatment. This enabled us to investigate PD-related changes of functional connectivity with STN that are not remedied by medical treatment. On the other hand, we might have missed other relevant information, especially concerning symptoms that are known to improve by dopaminergic treatment, and that might hence be only detectable in patients off medication. Moreover, medication induced adverse effects (e.g., levodopa-induced dyskinesia) might provoke additional activations and/or functional connections. To clearly identify pathophysiological functional connectivity changes that are reversible by medical treatment, direct comparison of the same patient sample in the medication-ON and -OFF states (and ideally also in a drug-naïve state) would be needed. Importantly, while all patients with PD received dopaminergic treatment, they were recruited from three sites without regard of the current medication scheme and without influencing medication for the purposes of the study. Hence, the exact choice and dosage of the medication in each patient was the result of individual optimization by the responsible neurologist at each site (see section "Sample"). Due to the diversity of possible combinations

of medication even within each site, we did not control for this potential source of variance in the patient group, and sub-analyses between patients with different medication status were beyond the scope of this study. Please note that a more heterogeneous medication in the patients' group will most likely lead to higher statistical variance, rendering it more difficult to detect significant functional connectivity differences between patients and controls. Compared to a setting with homogenous medication, we therefore argue that our analysis represents a more conservative and externally valid approach to identify PD-related differences in STN-connectivity in a medicated setting.

Since we were specifically interested in relations between changes in functional connectivity with STN and motor symptoms, no clinically relevant neuropsychological data was available at all three sites for correlation with connectivity strength of the STN. However, this could be interesting in future investigations, specifically in light of previously reported connections between STN and non-motor related regions [Hamani et al., 2004; Haynes and Haber, 2013; Temel et al., 2005]. Especially our hypothesis of greater interference between activity in motor and cognitive processing regions of the STN network needs to be corroborated by behavioral and cognitive performance data.

Conclusion

Our study on PD-related changes of the global functional connectivity with STN at "rest" revealed an attenuation of negative STN-coupling with Crus I of the cerebellum and medial prefrontal regions in patients with PD. Furthermore, bilateral IPS/SPC showed enhanced negative STN-coupling in patients with PD. IPS/SPC might be involved in compensatory mechanisms (related to impaired motor sequencing, e.g. in speech production) in PD, and enhanced negative coupling might be a way to protect compensatory brain regions from interference through pathological activity of the STN. Finally, with the progression of motor symptoms, we found a decline in positive STN-coupling of the left insula, which is a key region for executive function. Therefore, this uncoupling might be associated with well-known executive dysfunctions in PD. Moreover, considering the role of the insula within the salience network, uncoupling between insula and STN might also induce an insufficient setting of thresholds for the discrimination between relevant and irrelevant salient environmental stimuli, explaining observations of disturbed response control in PD.

In summary, our results indicate that PD induces protection of compensatory brain regions from interference through pathological STN-activity, and reduces coupling between STN and a key region for executive function.

REFERENCES

Amunts K, Schleicher A, Burgel U, Mohlberg H, Uylings HB, Zilles K (1999): Broca's region revisited: Cytoarchitecture and intersubject variability. J Comp Neurol 412:319–341.

Amunts K, Malikovic A, Mohlberg H, Schormann T, Zilles K (2000): Brodmann's areas 17 and 18 brought into stereotaxic space-where and how variable? Neuroimage 11:66–84.

Amunts K, Kedo O, Kindler M, Pieperhoff P, Mohlberg H, Shah NJ, Habel U, Schneider F, Zilles K (2005): Cytoarchitectonic mapping of the human amygdala, hippocampal region and entorhinal cortex: Intersubject variability and probability maps. Anat Embryol (Berl) 210:343–352.

Anticevic A, Cole MW, Murray JD, Corlett PR, Wang XJ, Krystal JH (2012): The role of default network deactivation in cognition and disease. Trends Cogn Sci 16:584–592.

Arnold C, Gehrig J, Gispert S, Seifried C, Kell CA (2013): Pathomechanisms and compensatory efforts related to Parkinsonian speech. Neuroimage Clin 4:82–97.

Aron AR, Behrens TE, Smith S, Frank MJ, Poldrack RA (2007): Triangulating a cognitive control network using diffusion-weighted magnetic resonance imaging (MRI) and functional MRI. J Neurosci 27:3743–3752.

Ashburner J, Friston KJ (2005): Unified segmentation. Neuroimage 26:839–851.

Baggio HC, Segura B, Sala-Llonch R, Marti MJ, Valldeoriola F, Compta Y, Tolosa E, Junque C (2015): Cognitive impairment and resting-state network connectivity in Parkinson's disease. Hum Brain Mapp 36:199–212.

Balsters JH, Laird AR, Fox PT, Eickhoff SB (2014): Bridging the gap between functional and anatomical features of cortico-cerebellar circuits using meta-analytic connectivity modeling. Hum Brain Mapp 35:3152–3169.

Baudrexel S, Witte T, Seifried C, von Wegner F, Beissner F, Klein JC, Steinmetz H, Deichmann R, Roeper J, Hilker R (2011): Resting state fMRI reveals increased subthalamic nucleus-motor cortex connectivity in Parkinson's disease. Neuroimage 55: 1728–1738.

Behrens TE, Johansen-Berg H, Woolrich MW, Smith SM, Wheeler-Kingshott CA, Boulby PA, Barker GJ, Sillery EL, Sheehan K Ciccarelli O, Thompson AJ, Brady JM, Matthews PM (2003): Non-invasive mapping of connections between human thalamus and cortex using diffusion imaging. Nat Neurosci 6:750–757.

Binder JR, Medler DA, Desai R, Conant LL, Liebenthal E (2005): Some neurophysiological constraints on models of word naming. Neuroimage 27:677–693.

Biswal B, Yetkin FZ, Haughton VM, Hyde JS (1995): Functional connectivity in the motor cortex of resting human brain using echo-planar MRI. Magn Reson Med 34:537–541.

Brittain JS, Watkins KE, Joundi RA, Ray NJ, Holland P, Green AL, Aziz TZ, Jenkinson N (2012): A role for the subthalamic nucleus in response inhibition during conflict. J Neurosci 32: 13396–13401.

Brunenberg EJ, Moeskops P, Backes WH, Pollo C, Cammoun L, Vilanova A, Janssen ML, Visser-Vandewalle VE, ter Haar Romeny BM, Thiran JP, Platel B (2012): Structural and resting state functional connectivity of the subthalamic nucleus: Identification of motor STN parts and the hyperdirect pathway. PloS One 7:e39061

Caspers S, Geyer S, Schleicher A, Mohlberg H, Amunts K, Zilles K (2006): The human inferior parietal cortex: Cytoarchitectonic

parcellation and interindividual variability. Neuroimage 33: 430–448.
Caspers S, Eickhoff SB, Geyer S, Scheperjans F, Mohlberg H, Zilles K, Amunts K (2008): The human inferior parietal lobule in stereotaxic space. Brain Struct Funct 212:481–495.
Castrioto A, Lhommee E, Moro E, Krack P (2014): Mood and behavioural effects of subthalamic stimulation in Parkinson's disease. Lancet Neurol 13:287–305.
Catalan MJ, Honda M, Weeks RA, Cohen LG, Hallett M (1998): The functional neuroanatomy of simple and complex sequential finger movements: A PET study. Brain 121:253–264.
Catalan MJ, Ishii K, Honda M, Samii A, Hallett M (1999): A PET study of sequential finger movements of varying length in patients with Parkinson's disease. Brain 122:483–495.
Choi HJ, Zilles K, Mohlberg H, Schleicher A, Fink GR, Armstrong E, Amunts K (2006): Cytoarchitectonic identification and probabilistic mapping of two distinct areas within the anterior ventral bank of the human intraparietal sulcus. J Comp Neurol 495:53–69.
Cieslik EC, Mueller VI, Eickhoff CR, Langner R, Eickhoff SB (2015): Three key regions for supervisory attentional control: Evidence from neuroimaging meta-analyses. Neurosci Biobehav Rev 48:22–34.
Cohen J. 1988. Statistical Power Analysis for the Behavioral Sciences. Hillsdale, NJ: L. Erlbaum Associates. 567 p.
Craig AD (2009): How do you feel now? The anterior insula and human awareness. Nat Rev Neurosci 10:59–70.
Darvas F, Hebb AO (2014): Task specific inter-hemispheric coupling in human subthalamic nuclei. Front Hum Neurosci 8: 701.
Diedrichsen J, Balsters JH, Flavell J, Cussans E, Ramnani N (2009): A probabilistic MR atlas of the human cerebellum. Neuroimage 46:39–46.
Eickhoff SB, Amunts K, Mohlberg H, Zilles K (2006a): The human parietal operculum. II. Stereotaxic maps and correlation with functional imaging results. Cereb Cortex 16:268–279.
Eickhoff SB, Schleicher A, Zilles K, Amunts K (2006b): The human parietal operculum. I. Cytoarchitectonic mapping of subdivisions. Cereb Cortex 16:254–267.
Eickhoff SB, Paus T, Caspers S, Grosbras MH, Evans AC, Zilles K, Amunts K (2007): Assignment of functional activations to probabilistic cytoarchitectonic areas revisited. Neuroimage 36: 511–521.
Fernandez-Seara MA, Mengual E, Vidorreta M, Castellanos G, Irigoyen J, Erro E, Pastor MA (2015): Resting state functional connectivity of the subthalamic nucleus in Parkinson's disease assessed using arterial spin-labeled perfusion fMRI. Hum Brain Mapp 36:1937–1950.
Fox MD, Snyder AZ, Vincent JL, Corbetta M, Van Essen DC, Raichle ME (2005): The human brain is intrinsically organized into dynamic, anticorrelated functional networks. Proc Natl Acad Sci USA 102:9673–9678.
Frank MJ (2006): Hold your horses: A dynamic computational role for the subthalamic nucleus in decision making. Neural Netw 19:1120–1136.
Frank MJ, Samanta J, Moustafa AA, Sherman SJ (2007): Hold your horses: Impulsivity, deep brain stimulation, and medication in parkinsonism. Science 318:1309–1312.
Fransson P (2005): Spontaneous low-frequency BOLD signal fluctuations: An fMRI investigation of the resting-state default mode of brain function hypothesis. Hum Brain Mapp 26:15–29.
Geyer S (2004): The microstructural border between the motor and the cognitive domain in the human cerebral cortex. Adv Anat Embryol Cell Biol 174:1–89.
Geyer S, Ledberg A, Schleicher A, Kinomura S, Schormann T, Burgel U, Klingberg T, Larsson J, Zilles K, Roland PE (1996): Two different areas within the primary motor cortex of man. Nature 382:805–807.
Geyer S, Schleicher A, Zilles K (1999): Areas 3a, 3b, and 1 of human primary somatosensory cortex. Neuroimage 10:63–83.
Geyer S, Schormann T, Mohlberg H, Zilles K (2000): Areas 3a, 3b, and 1 of human primary somatosensory cortex. II. Spatial normalization to standard anatomical space. Neuroimage 11:684–696.
Goodkind M, Eickhoff SB, Oathes DJ, Jiang Y, Chang A, Jones-Hagata LB, Ortega BN, Zaiko YV, Roach EL, Korgaonkar MS, Grieve SM, Galatzer-Levy I, Fox PT, Etkin A (2015): Identification of a common neurobiological substrate for mental illness. JAMA Psychiatry 72:305–315.
Grefkes C, Geyer S, Schormann T, Roland P, Zilles K (2001): Human somatosensory area 2: Observer-independent cytoarchitectonic mapping, interindividual variability, and population map. Neuroimage 14:617–631.
Grefkes C, Ritzl A, Zilles K, Fink GR (2004): Human medial intraparietal cortex subserves visuomotor coordinate transformation. Neuroimage 23:1494–1506.
Greicius MD, Krasnow B, Reiss AL, Menon V (2003): Functional connectivity in the resting brain: A network analysis of the default mode hypothesis. Proc Natl Acad Sci USA 100:253–258.
Hamani C, Saint-Cyr JA, Fraser J, Kaplitt M, Lozano AM (2004): The subthalamic nucleus in the context of movement disorders. Brain 127:4–20.
Haynes WI, Haber SN (2013): The organization of prefrontal-subthalamic inputs in primates provides an anatomical substrate for both functional specificity and integration: Implications for Basal Ganglia models and deep brain stimulation. J Neurosci 33:4804–4814.
Hebb AO, Darvas F, Miller KJ (2012): Transient and state modulation of beta power in human subthalamic nucleus during speech production and finger movement. Neuroscience 202: 218–233.
Heim S, Amunts K, Hensel T, Grande M, Huber W, Binkofski F, Eickhoff SB (2012): The role of human parietal area 7A as a link between sequencing in hand actions and in overt speech production. Front Psychol 3:534.
Hughes AJ, Daniel SE, Kilford L, Lees AJ (1992): Accuracy of clinical diagnosis of idiopathic Parkinson's disease: A clinico-pathological study of 100 cases. J Neurol Neurosurg Psychiatry 55:181–184.
Ibarretxe-Bilbao N, Ramirez-Ruiz B, Junque C, Marti MJ, Valldeoriola F, Bargallo N, Juanes S, Tolosa E (2010): Differential progression of brain atrophy in Parkinson's disease with and without visual hallucinations. J Neurol Neurosurg Psychiatry 81:650–657.
Ibarretxe-Bilbao N, Junque C, Marti MJ, Tolosa E (2011): Cerebral basis of visual hallucinations in Parkinson's disease: Structural and functional MRI studies. J Neurol Sci 310:79–81.
Jakobs O, Langner R, Caspers S, Roski C, Cieslik EC, Zilles K, Laird AR, Fox PT, Eickhoff SB (2012): Across-study and within-subject functional connectivity of a right temporo-parietal junction subregion involved in stimulus-context integration. Neuroimage 60:2389–2398.

Kehagia AA, Barker RA, Robbins TW (2010): Neuropsychological and clinical heterogeneity of cognitive impairment and dementia in patients with Parkinson's disease. Lancet Neurol 9:1200–1213.

Keller CJ, Bickel S, Honey CJ, Groppe DM, Entz L, Craddock RC, Lado FA, Kelly C, Milham M, Mehta AD (2013): Neurophysiological investigation of spontaneous correlated and anticorrelated fluctuations of the BOLD signal. J Neurosci 33:6333–6342.

Kelly AM, Uddin LQ, Biswal BB, Castellanos FX, Milham MP (2008): Competition between functional brain networks mediates behavioral variability. Neuroimage 39:527–537.

Kelly C, Toro R, Di Martino A, Cox CL, Bellec P, Castellanos FX, Milham MP (2012): A convergent functional architecture of the insula emerges across imaging modalities. Neuroimage 61: 1129–1142.

Klepac N, Trkulja V, Relja M, Babic T (2008): Is quality of life in non-demented Parkinson's disease patients related to cognitive performance? A clinic-based cross-sectional study. Eur J Neurol 15:128–133.

Kuhn AA, Tsui A, Aziz T, Ray N, Brucke C, Kupsch A, Schneider GH, Brown P (2009): Pathological synchronisation in the subthalamic nucleus of patients with Parkinson's disease relates to both bradykinesia and rigidity. Exp Neurol 215:380–387.

Kurani AS, Seidler RD, Burciu RG, Comella CL, Corcos DM, Okun MS, MacKinnon CD, Vaillancourt DE (2015): Subthalamic nucleus–sensorimotor cortex functional connectivity in de novo and moderate Parkinson's disease. Neurobiol Aging 36: 462–469.

Kurth F, Eickhoff SB, Schleicher A, Hoemke L, Zilles K, Amunts K (2010a): Cytoarchitecture and probabilistic maps of the human posterior insular cortex. Cereb Cortex 20:1448–1461.

Kurth F, Zilles K, Fox PT, Laird AR, Eickhoff SB (2010b): A link between the systems: Functional differentiation and integration within the human insula revealed by meta-analysis. Brain Struct Funct 214:519–534.

Liu H, Edmiston EK, Fan G, Xu K, Zhao B, Shang X, Wang F (2013): Altered resting-state functional connectivity of the dentate nucleus in Parkinson's disease. Psychiatry Res 211:64–71.

Lopez-Azcarate J, Tainta M, Rodriguez-Oroz MC, Valencia M, Gonzalez R, Guridi J, Iriarte J, Obeso JA, Artieda J, Alegre M (2010): Coupling between beta and high-frequency activity in the human subthalamic nucleus may be a pathophysiological mechanism in Parkinson's disease. J Neurosci 30:6667–6677.

Magri C, Schridde U, Murayama Y, Panzeri S, Logothetis NK (2012): The amplitude and timing of the BOLD signal reflects the relationship between local field potential power at different frequencies. J Neurosci 32:1395–1407.

Malikovic A, Amunts K, Schleicher A, Mohlberg H, Eickhoff SB, Wilms M, Palomero-Gallagher N, Armstrong E, Zilles K (2007): Cytoarchitectonic analysis of the human extrastriate cortex in the region of V5/MT+: A probabilistic, stereotaxic map of area hOc5. Cereb Cortex 17:562–574.

Mansfield EL, Karayanidis F, Jamadar S, Heathcote A, Forstmann BU (2011): Adjustments of response threshold during task switching: A model-based functional magnetic resonance imaging study. J Neurosci 31:14688–14692.

Matar E, Shine JM, Naismith SL, Lewis SJ (2013): Using virtual reality to explore the role of conflict resolution and environmental salience in freezing of gait in Parkinson's disease. Parkinsonism Relat Disord 19:937–942.

Mathys C, Hoffstaedter F, Caspers J, Caspers S, Sudmeyer M, Grefkes C, Eickhoff SB, Langner R (2014): An age-related shift of resting-state functional connectivity of the subthalamic nucleus: A potential mechanism for compensating motor performance decline in older adults. Front Aging Neurosci 6:178

Menon V, Uddin LQ (2010): Saliency, switching, attention and control: A network model of insula function. Brain Struct Funct 214:655–667.

Michely J, Volz LJ, Barbe MT, Hoffstaedter F, Viswanathan S, Timmermann L, Eickhoff SB, Fink GR, Grefkes C (2015): Dopaminergic modulation of motor network dynamics in Parkinson's disease. Brain 138:664–678.

Morosan P, Rademacher J, Schleicher A, Amunts K, Schormann T, Zilles K (2001): Human primary auditory cortex: Cytoarchitectonic subdivisions and mapping into a spatial reference system. Neuroimage 13:684–701.

Movement Disorder Society Task Force on Rating Scales for Parkinson's (2003): The Unified Parkinson's Disease Rating Scale (UPDRS): Status and recommendations. Mov Disord 18:738–750.

Müller VI, Langner R, Cieslik EC, Rottschy C, Eickhoff SB (2015): Interindividual differences in cognitive flexibility: influence of gray matter volume, functional connectivity and trait impulsivity. Brain Struct Funct 220:2401–2414.

Murphy K, Birn RM, Handwerker DA, Jones TB, Bandettini PA (2009): The impact of global signal regression on resting state correlations: Are anti-correlated networks introduced? Neuroimage 44:893–905.

Nambu A, Tokuno H, Takada M (2002): Functional significance of the cortico-subthalamo-pallidal 'hyperdirect' pathway. Neurosci Res 43:111–117.

Nishio Y, Hirayama K, Takeda A, Hosokai Y, Ishioka T, Suzuki K, Itoyama Y, Takahashi S, Mori E (2010): Corticolimbic gray matter loss in Parkinson's disease without dementia. Eur J Neurol 17:1090–1097.

Novak P, Klemp JA, Ridings LW, Lyons KE, Pahwa R, Nazzaro JM (2009): Effect of deep brain stimulation of the subthalamic nucleus upon the contralateral subthalamic nucleus in Parkinson disease. Neurosci Lett 463:12–16.

Power JD, Mitra A, Laumann TO, Snyder AZ, Schlaggar BL, Petersen SE (2014): Methods to detect, characterize, and remove motion artifact in resting state fMRI. Neuroimage 84: 320–341.

Power JD, Schlaggar BL, Petersen SE (2015): Recent progress and outstanding issues in motion correction in resting state fMRI. Neuroimage 105:536–551.

Putcha D, Ross RS, Cronin-Golomb A, Janes AC, Stern CE (2015): Altered intrinsic functional coupling between core neurocognitive networks in Parkinson's disease. Neuroimage Clin 7:449–455.

Reetz K, Dogan I, Rolfs A, Binkofski F, Schulz JB, Laird AR, Fox PT, Eickhoff SB (2012): Investigating function and connectivity of morphometric findings—Exemplified on cerebellar atrophy in spinocerebellar ataxia 17 (SCA17). Neuroimage 62:1354–1366.

Rektorova I, Krajcovicova L, Marecek R, Novakova M, Mikl M (2014): Default mode network connectivity patterns associated with visual processing at different stages of Parkinson's disease. J Alzheimers Dis 42:S217–S228.

Rizzone MG, Fasano A, Daniele A, Zibetti M, Merola A, Rizzi L, Piano C, Piccininni C, Romito LM Lopiano L, Albanese A (2014): Long-term outcome of subthalamic nucleus DBS in Parkinson's disease: From the advanced phase towards the late stage of the disease? Parkinsonism Relat Disord 20:376–381.

Rochester L, Galna B, Lord S, Burn D (2014): The nature of dual-task interference during gait in incident Parkinson's disease. Neuroscience 265:83–94.

Rorden C, Brett M (2000): Stereotaxic display of brain lesions. Behav Neurol 12:191–200.

Roski C, Caspers S, Langner R, Laird AR, Fox PT, Zilles K, Amunts K, Eickhoff SB (2013): Adult age-dependent differences in resting-state connectivity within and between visual-attention and sensorimotor networks. Front Aging Neurosci 5: 67.

Rottschy C, Eickhoff SB, Schleicher A, Mohlberg H, Kujovic M, Zilles K, Amunts K (2007): Ventral visual cortex in humans: Cytoarchitectonic mapping of two extrastriate areas. Hum Brain Mapp 28:1045–1059.

Rottschy C, Kleiman A, Dogan I, Langner R, Mirzazade S, Kronenbuerger M, Werner C, Shah NJ, Schulz JB, Eickhoff SB, Reetz K (2013): Diminished activation of motor working-memory networks in Parkinson's disease. PLoS One 8:e61786.

Saad ZS, Gotts SJ, Murphy K, Chen G, Jo HJ, Martin A, Cox RW (2012): Trouble at rest: How correlation patterns and group differences become distorted after global signal regression. Brain Connect 2:25–32.

Saad ZS, Reynolds RC, Jo HJ, Gotts SJ, Chen G, Martin A, Cox RW (2013): Correcting brain-wide correlation differences in resting-state FMRI. Brain Connect 3:339–352.

Satterthwaite TD, Wolf DH, Ruparel K, Erus G, Elliott MA, Eickhoff SB, Gennatas ED, Jackson C, Prabhakaran K, Smith A, Hakonarson H, Verma R, Davatzikos C, Gur RE, Gur RC (2013): Heterogeneous impact of motion on fundamental patterns of developmental changes in functional connectivity during youth. Neuroimage 83:45–57.

Schafer A, Forstmann BU, Neumann J, Wharton S, Mietke A, Bowtell R, Turner R (2012): Direct visualization of the subthalamic nucleus and its iron distribution using high-resolution susceptibility mapping. Hum Brain Mapp 33:2831–2842.

Scheperjans F, Eickhoff SB Homke L, Mohlberg H, Hermann K, Amunts K, Zilles K, (2008a): Probabilistic maps, morphometry, and variability of cytoarchitectonic areas in the human superior parietal cortex. Cereb Cortex 18:2141–2157.

Scheperjans F, Hermann K, Eickhoff SB, Amunts K, Schleicher A, Zilles K (2008b): Observer-independent cytoarchitectonic mapping of the human superior parietal cortex. Cereb Cortex 18: 846–867.

Seeley WW, Menon V, Schatzberg AF, Keller J, Glover GH, Kenna H, Reiss AL, Greicius MD (2007): Dissociable intrinsic connectivity networks for salience processing and executive control. J Neurosci 27:2349–2356.

Shine JM, Halliday GM, Gilat M, Matar E, Bolitho SJ, Carlos M, Naismith SL, Lewis SJ (2014): The role of dysfunctional attentional control networks in visual misperceptions in Parkinson's disease. Hum Brain Mapp 35:2206–2219.

Shulman GL, Astafiev SV, Franke D, Pope DL, Snyder AZ, McAvoy MP, Corbetta M (2009): Interaction of stimulus-driven reorienting and expectation in ventral and dorsal frontoparietal and basal ganglia-cortical networks. J Neurosci 29:4392–4407.

Skidmore FM, Yang M, Baxter L, von Deneen KM, Collingwood J, He G, White K, Korenkevych D, Savenkov A, Heilman KM, Gold M, Liu Y (2013): Reliability analysis of the resting state can sensitively and specifically identify the presence of Parkinson disease. Neuroimage 75:249–261.

Spreng RN, Stevens WD, Chamberlain JP, Gilmore AW, Schacter DL (2010): Default network activity, coupled with the frontoparietal control network, supports goal-directed cognition. Neuroimage 53:303–317.

Temel Y, Blokland A, Steinbusch HW, Visser-Vandewalle V (2005): The functional role of the subthalamic nucleus in cognitive and limbic circuits. Prog Neurobiol 76:393–413.

Tomlinson CL, Stowe R, Patel S, Rick C, Gray R, Clarke CE (2010): Systematic review of levodopa dose equivalency reporting in Parkinson's disease. Mov Disord 25:2649–2653.

Uddin LQ, Kelly AM, Biswal BB, Castellanos FX, Milham MP (2009): Functional connectivity of default mode network components: Correlation, anticorrelation, and causality. Hum Brain Mapp 30:625–637.

Van Dijk KR, Sabuncu MR, Buckner RL (2012): The influence of head motion on intrinsic functional connectivity MRI. Neuroimage 59:431–438.

Volkmann J (2007): Update on surgery for Parkinson's disease. Curr Opin Neurol 20:465–469.

Walker HC, Watts RL, Schrandt CJ, Huang H, Guthrie SL, Guthrie BL, Montgomery EB Jr. (2011): Activation of subthalamic neurons by contralateral subthalamic deep brain stimulation in Parkinson disease. J Neurophysiol 105:1112–1121.

Weintraub DB, Zaghloul KA (2013): The role of the subthalamic nucleus in cognition. Rev Neurosci 24:125–138.

Wild LB, de Lima DB, Balardin JB, Rizzi L, Giacobbo BL, Oliveira HB, de Lima A, II, Peyre-Tartaruga LA, Rieder CR, Bromberg E (2013): Characterization of cognitive and motor performance during dual-tasking in healthy older adults and patients with Parkinson's disease. J Neurol 260:580–589.

Winstein CJ, Grafton ST, Pohl PS (1997): Motor task difficulty and brain activity: Investigation of goal-directed reciprocal aiming using positron emission tomography. J Neurophysiol 77:1581–1594.

Wu T, Hallett M (2013): The cerebellum in Parkinson's disease. Brain 136:696–709.

Wu T, Long X, Wang L, Hallett M, Zang Y, Li K, Chan P (2011): Functional connectivity of cortical motor areas in the resting state in Parkinson's disease. Hum Brain Mapp 32:1443–1457.

Wu T, Liu J, Hallett M, Zheng Z, Chan P (2013): Cerebellum and integration of neural networks in dual-task processing. Neuroimage 65:466–475.

Yamamoto R, Iseki E, Murayama N, Minegishi M, Marui W, Togo T, Katsuse O, Kosaka K, Kato M, Iwatsubo T, Arai H (2007): Correlation in Lewy pathology between the claustrum and visual areas in brains of dementia with Lewy bodies. Neurosci Lett 415:219–224.

Ye Z, Altena E, Nombela C, Housden CR, Maxwell H, Rittman T, Huddleston C, Rae CL, Regenthal R, Sahakian BJ, Barker RA, Robbins TW, Rowe JB (2014): Selective serotonin reuptake inhibition modulates response inhibition in Parkinson's disease. Brain 137:1145–1155.

Yu R, Liu B, Wang L, Chen J, Liu X (2013): Enhanced functional connectivity between putamen and supplementary motor area in Parkinson's disease patients. PLoS One 8:e59717.

Zarahn E, Aguirre GK, D'Esposito M (1997): Empirical analyses of BOLD fMRI statistics. I. Spatially unsmoothed data collected under null-hypothesis conditions. Neuroimage 5:179–197.

Zilles K, Amunts K (2010): Centenary of Brodmann's map—Conception and fate. Nat Rev Neurosci 11:139–145.